Proceedings of 7th Transport Research Arena TRA 2018, April 16-19, 2018, Vienna, Austria

Cooling Fluids and Ambient Temperature: Sensitivity Performance of a Container Ship Organic Rankine Cycle Unit

Santiago Suárez de la Fuente [a], Ulrik Larsen [b], Richard Bucknall [a], Alistair Greig [a]*

[a] *University College London, Department of Mechanical Engineering, London, Roberts Building, Torrington Place , WC1E 7JE, United Kingdom*

[b] *Chalmers University of Technology, Maritime Operations, 412 96 Gothenburg, Sweden*

Abstract

The objective of this paper is to design organic Rankine cycle units that are cooled by air or seawater and show the changes in net power output and power requirement as the ambient air temperatures change both geographically and seasonally. The organic Rankine cycle unit uses the available waste heat from the scavenge air system for a 4,100 TEU container ship. This work uses a two-step single objective optimisation capable of selecting 14 design characteristics of the organic Rankine cycle unit and with the aim of minimising the vessel's CO_2 emissions. The work contributes to the study of off-design operation and different cooling fluids for marine waste heat recovery systems. The results show that the organic Rankine cycle unit is more adaptable to ambient air temperatures when using seawater as a cooling fluid while air is an attractive option for extremely low ambient temperatures.

Keywords: Cooling fluid, Ship, Waste heat recovery system, CO_2 emissions, Ambient air temperature.

* Corresponding author. Tel.: +44 207 679 3895
E-mail address: a_greig@meng.ucl.ac.uk

Nomenclature

Latin symbols		
A	Area,	m^2
C_p	Specific heat,	kJ/(kg K)
CF	Carbon factor,	g CO_2/g fuel
CS	Carbon savings,	t
d	Diameter,	m
F	Correction factor,	-
h	Specific enthalpy,	kJ/kg
h^*	Convective heat transfer coefficient,	kW/(m^2 K)
$\dot{Q}$	Heat flux,	kW
T	Temperature,	K (°C)
t	Time,	hours
U	Overall heat transfer coefficient,	kW/(m^2 K)
$\dot{W}$	Power,	kW

Greek symbols		
η	Efficiency,	-
κ	Thermal conductivity,	kW/(m K)

Subscripts and superscripts	
AE	Auxiliary engine
C	Cold
co	Condenser
d	Design point
ds	Desuperheater
e	Electrical
ev	Evaporator
f	Fins
Gen	Generator
H	Hot
i	In or inlet
o	Out or outlet
p	Pump
ph	Preheater
pp	Pinch Point
S	Coolant
sh	Superheater
T	Total
t	Tube
wf	Working fluid

1. Introduction

Waste heat recovery systems (WHRS) are one of the preferable energy efficiency enhancing devices (EEED) among ship owners being installed on board. Larsen, Haglind, et al. (2013) showed that a marine WHRS could increase the power production on board by 5%; Suárez de la Fuente et al. (2017) demonstrated that it is possible to generate about 325 kW of electricity on board 107,000 deadweight tonnage tanker; and MAN Diesel and Turbo gives a figure for recoverable power between 5% and 8% for dual-pressure water-based Rankine cycle. An interesting source of waste heat is the scavenge air system which, depending on the engine, could represent about 17% of the waste heat in a two-stroke slow speed Diesel engine (Woodyard 2009; MAN Diesel & Turbo 2012). Scavenge air system waste heat is under usual operating conditions available at temperatures between 100°C and 200°C which is suitable for an Organic Rankine cycle (ORC) unit.

Air and seawater are two readily heat sinks for the marine WHRS. Normally, air is not considered due to its lower heat transfer coefficient resulting in larger heat transfer areas and volumetric flows in comparison to seawater (Bustamante et al. 2016) but in colder climates air offers the potential for significantly greater temperature differential.

An important aspect of shipping is the wide range of operating conditions (Banks et al. 2013) which depend on days at sea, type of cargo and ship loading, among others. Also, ships can navigate several different oceans within the same route but also they sail during the whole year, facing different weather conditions. The ship and its on board systems are normally designed to operate at its maximum efficiency at a particular design condition which, in operative life, seldom occurs. This presents a challenge to ship owners when trying to choose EEED, such as WHRS, to improve the ship performance and reduce its noxious emissions.

The performance change of marine WHRS due to different operating characteristics has been explored by the literature. Yang and Yeh (2015) showed how the thermal efficiency of different ORC increases as the coolant temperature reduces; while not considering the power consumption related to the condenser coolant. Suárez de la Fuente and Greig (2015) quantified the performance and annual CO_2 emission reductions for five marine WHRS under a varying profile requiring different engine loading conditions. Livanos et al. (2014) present the power returned by a marine WHRS at different main engine loadings.

2. Case Study

2.1. The Ship

In this study a hypothetical 4,130 twenty-foot equivalent unit (TEU) container ship based on the *JPO Libra* is used (Clarkson Research Services Limited 2013). The vessel's resistance and propulsive power demand at different speeds are calculated using UCL's Whole Ship Model (WSM) which is an evolution from the Ship Impact Model (Calleya et al. 2015). Table 1 presents a combination of characteristics used and calculated by WSM for the studied vessel. Table 2 shows the vessel's power-speed distribution, the impact of sea state is not considered. The vessel is powered by a two-stroke slow speed Diesel engine using heavy fuel oil (HFO). The design point is set at 75% of its Maximum Continuous Rating (MCR) with a power output of 30,840 kW and a specific fuel oil consumption (SFOC) of 159 g/kWh (MAN Diesel & Turbo 2015). On the auxiliary side, a constant electric demand of 1,390 kW_e is taken from Smith et al. (2014) with an assumed auxiliary engine SFOC at design point of 227 g/kWh. It is also assumed that the auxiliary engine is operating with an engine margin of 15% which gives a total installed power of 1,635 kW_e. As the ship navigates across different oceans and at different seasons, the change in the ambient temperature modifies the engine behaviour. Fig. 1 shows how the main engine scavenge air characteristics vary with ambient air temperature. Seldom will a ship be operating at its design conditions which creates a challenge when designing a marine WHRS since the waste heat availability and temperature will be always changing (particularly the scavenge air heat).

Table 1. Container vessel's characteristics used for the case study (Clarkson Research Services Limited 2013).

Design Speed (kn)	Deadweight (t)	Length (m)	Beam (m)	Draught (m)	Midship Coefficient (-)	Prismatic Coefficient (-)
23.3	52,450	252	32.2	12.5	0.981	0.653

Table 2. Operating profile for the hypothetical containership.

Speed (kn)	Power Required (kW)	Time (%)	mcr (%)
25.2	41,150	<1.0	100
24.6	37,550	4.0	90
23.3	30,840 (design point)	12.8	75
22.1	25,210	15.5	60
21.1	20,925	20.3	50
19.8	16,810	12.6	40
<18.6	<13,730	34.8	33

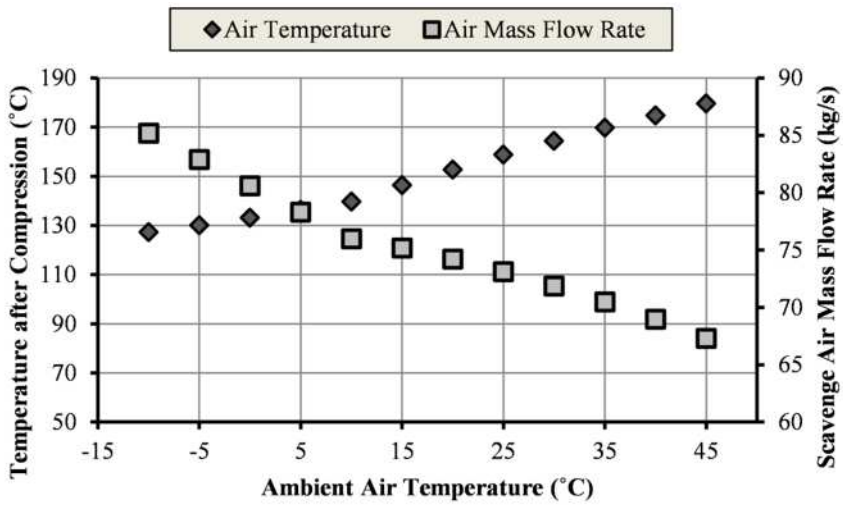

Fig. 1. Scavenge air temperature (right) and mass flow rate (left) at different ambient air temperatures and a constant engine loading of 75% MCR (MAN Diesel & Turbo 2015).

2.2. Waste heat recovery system

While the two-stroke main engine is in operation, air enters the turbocharger's compressor increasing its pressure but also its temperature which in turn reduces the air's density. The air temperature after compression is cooled via the WHRS boiler. Before the inlet air enters the engine, a secondary cooler will subsequently cool the air to the required temperatures by the engine manufacturer (MAN Diesel & Turbo 2015). Referring to Fig. 2, the high pressure and temperature working fluid enters the expander (1) and provides mechanical power due to the expansion process. An electrical generator is connected via a gearbox to the expander's shaft to transform the mechanical power to electrical power. The condenser unit (2-3) condenses the working fluid at constant pressure by rejecting heat to the sink, having at the end of the process, as an assumption, a saturated liquid. At point 3, the saturated liquid is pumped to the boiler (4). Inside the boiler (4-1), the working fluid absorbs the available waste heat increasing the working fluid's temperature to reach the same conditions as for point 1. With the intention of minimising the ORC unit size impact, the maximum power output from the turbine is limited to 600 kW and a maximum condenser volume of 38.5 m^3 equivalent to the volume of one TEU. This was chosen as an easily understood reference volume. The potential exists to fit a much larger condenser but the ship impact needs to be considered.

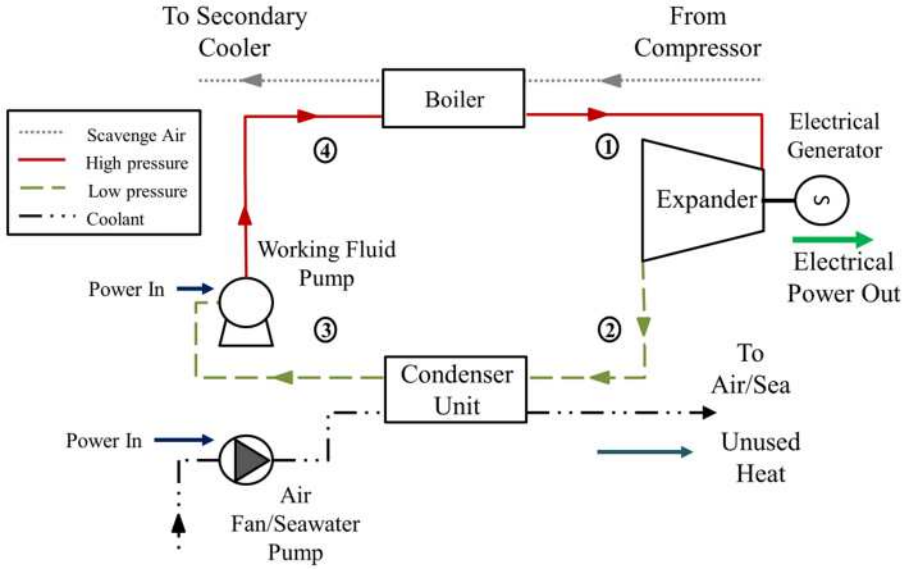

Fig. 2. ORC unit plant layout using the available waste heat in the scavenge air system.

The selected working fluid for the marine ORC unit is R1233zd(E) (see Table 3), because it is classified as non-flammable (Honeywell 2014) and hence it is allowed inside the machinery room (International Maritime Organization 2009), and being capable of operating under the scavenge air temperatures (Datla & Brasz 2014). The WHRS model will prevent the optimisation process from selecting a superheating temperature equal or larger than the refrigerant decomposition temperature. Another relevant characteristic from this fluid is that it has a low 100 years Global Warming Potential (GWP_{100}).

Table 3. Working fluid's characteristics.

Working Fluid	Fluid Group[a]	GWP_{100} (-)[b]	ODP (-)[c]	Auto-ignition Temp. (˚C)[d]	Decomposition Temp. (˚C)[e]	T_{cr} (˚C)[g]	P_{cr} (MPa)[g]
R1233zd(E)	Hydrochlorofluoroolefin	<5	0.0	380	175	167	3.62

[a] Molés et al. (2014); [b,c] Hulse et al.(2012); [d,f] Honeywell (2014); [e] Kontomaris (2014); [g] Lemmon et al. (2010).

When seawater is used as coolant for the ORC a shell and tube heat exchanger will be used since they offer great flexibility in design and they are suitable for a liquid coolant (Sinnott 2005). Also the ease of maintenance makes it an attractive option since using seawater will require constant and specialised maintenance to reduce bio-fouling. Seawater will be flowing inside the tubes while outside, in counter flow, the organic fluid will be condensing. The tube layout chosen is a rotated square and due to seawater's corrosiveness, the material used is stainless steel.

For air, a cross-flow finned tube heat exchanger will be used as it offers high heat transfer area densities reducing its mass and volume. The working fluid will be flowing inside the tubes while air will be moving in the finned

side. Another advantage of this arrangement is that it improves the overall heat transfer coefficient (*U*) since the large heat transfer area compensates for air's low convective heat transfer coefficient (*h**). The finned tube condenser unit is made of aluminium with five tube rows with a constant transverse pitch (p_t) of 0.083 m.

Main and auxiliary engines are normally matched for one of three different ambient conditions for their SFOC (MAN Diesel & Turbo 2014a): Tropical at 45°C, ISO at 25°C or Winter at 10°C. As ambient air temperatures changes also the inlet air and maximum combustion pressures also change having an impact on the SFOC and waste heat availability(MAN Diesel & Turbo 2014b). The ship engines' power rate given at any ambient condition is valid for ambient air temperatures between -10˚C and 45˚C. The three ambient temperatures will be used to design the marine ORC unit. The CRUTEM4 and HadSST2 data sets (Jones et al. 1999; Rayner et al. 2006; Jones et al. 2012) were used to find the air and sea monthly temperatures for the different seas.

3. Method

3.1. Waste heat recovery system

The heat flow available from the scavenge air system ($\dot{Q}_H$) is defined as follows:

$$\dot{Q}_H = \dot{Q}_{ph} + \dot{Q}_{ev} + \dot{Q}_{sh} = \dot{m}_H \cdot C_{p\_H} \cdot \left(T_{H,i} - T_{H,o}\right) \quad (1)$$

Where the suffixes *ph*, *ev* and *sh* stand for boiler's subsections: preheater, evaporator and superheater respectively. The scavenge air mass flow rate entering the ORC boiler is represented by $\dot{m}_H$, C_{p_H} is the air's specific heat and $T_{H,i}$ and $T_{H,o}$ are the boiler's inlet and outlet temperature. Equating the heat leaving the exhaust gas to the heat absorbed by the working fluid is possible to determine the mass flow rate:

$$\dot{m}_{wf} = \frac{\dot{Q}_{ph}}{(h_{4a} - h_4)} \quad (2)$$

Where h_4 is the enthalpy before entering the boiler, h_{4a} is working fluid's enthalpy inside the boiler at the saturated liquid point and; $\dot{m}_{wf}$ is the working fluid mass flow rate. The power output of the expander ($\dot{W}_o$) is given by:

$$\dot{W}_o = \dot{m}_{wf} \cdot (h_1 - h_{2s}) \cdot \eta_{exp} \quad (3)$$

Where h_1 and h_{2s} are the specific enthalpy before and after an isentropic expansion, η_{exp} is the isentropic efficiency, assumed to be 80% at design point. The expander's shaft is connected to an electrical generator which has a constant efficiency (η_e) of 97%. The power input of the working fluid's pump ($\dot{W}_i$) is given by:

$$\dot{W}_i = \frac{\dot{m}_{wf} \cdot (h_3 - h_{4s})}{\eta_p} \quad (4)$$

Where h_3 is the working fluid specific enthalpies after the condenser unit, h_{4s} is the enthalpy at high pressure after an isentropic compression. The pump's isentropic efficiency (η_p) is assumed to be 80% at design point.

3.2. Condenser unit heat transfer

For the condenser unit, the heat rejected ($\dot{Q}_C$) to the coolant is given by:

$$\dot{Q}_C = \dot{Q}_{ds} + \dot{Q}_{co} = \dot{m}_{wf} \cdot [(h_3 - h_{2a}) - (h_{2a} - h_2)] \quad (5)$$

Where $\dot{Q}_{ds}$ and $\dot{Q}_{co}$ are the heat transferred in the condenser unit's desuperheating and condenser regions respectively; h_2 is the working fluid's specific enthalpy before the condenser unit and h_{2a} is the specific enthalpy at the vapour saturation point.

Looking into more detail and only for the condenser unit's condenser (*c*) section, the heat transfer phenomena across a surface can be defined by:

$$\dot{Q}_{co} = U_{co} \cdot A_{co} \cdot F_{cf} \cdot \Delta T_{lm,co} \quad (6)$$

Where $\dot{Q}$ is the heat rate, *U* is the overall heat transfer coefficient, *A* is the heat transfer area, F_{cf} is the temperature correction factor which accounts for the deviation of the flow shape inside the condenser unit from an ideal counter current flow and is calculated using the correlations given in the references listed in Table 4, and ΔT_{lm} is the

logarithm mean temperature difference. The overall heat transfer coefficient, seen from outside of a finned tube in the condensing region, is given as:

$$U_{co} = \frac{1}{\frac{1}{\eta_f A_{T,co}} \cdot \left(\frac{1}{h^*_{co,o}} + \frac{1}{h^*_{of}}\right) + \frac{d_o}{2\kappa_t} \cdot ln\left(\frac{d_o}{d_i}\right) + \frac{1}{A_{t,co}} \cdot \left(\frac{1}{h^*_{co,i}} + \frac{1}{h^*_{if}}\right)} \quad (7)$$

Table 4: Overview of used references for designing the WHRS condenser unit.

Section	Phenomena	Shell and Tube	Finned Tube
Coolant	Heat Transfer	Sinnott (2005)	Wang et al. (1999)
	Fin Efficiency	-	Schmidt (1949)
	Friction	Sinnott (2005)	Wang et al. (1999)
Working Fluid	Heat Transfer	Sinnott (2005), Gnielinski (1976)	Shah (1979), Gnielinski (1976)
	Friction	Sinnott (2005)	Petukhov (1970), Müller-Steinhagen and Heck (1986)
Condenser Unit	Temperature Correction Factor	Fakheri (2003)	Shah and Sekulic (2003)

The fin's efficiency is given by η_f, and κ_t is the thermal conductivity of the tube; A_T is the total heat transfer area in the desuperheating section which is the total fin's surface area (A_f) plus the tube's total free surface area (A_t). The internal and external tube's diameters are represented by d_i and d_o respectively. The fouling convective factors are represented by h^*_{if} and h^*_{of} – inside and outside of the tube – with a value of 5 kW/m^2·K. The variables $h^*_{ds,i}$ and $h^*_{ds,o}$ are the convective heat transfer coefficients for the inside and outside of the tube respectively and are found in the references given in Table 4. For the case of the shell and tube with bare tubes the terms A_T and η_f are removed. The coolant mass flow rate ($\dot{m}_S$) is calculated as follows:

$$\dot{m}_S = \frac{\dot{Q}_{co}}{C_{p\_C} \cdot \left(T_{2a} + \Delta T_{pp,C} - T_{S,i}\right)} \quad (8)$$

Where C_{p_C} is the coolants specific heat, T_{2a} is the working fluid saturation temperature, $\Delta T_{pp,C}$ is the condenser unit pinch point temperature difference and $T_{S,i}$ is the coolant inlet temperature. The pump or fan power consumption is given by:

$$\dot{W}_{i,S} = \frac{\dot{m}_S \cdot \left(h_{S,i} - h_{S,pp}\right)}{\eta_{p,S}} \quad (9)$$

Where $h_{S,i}$ and $h_{S,pp}$ are the specific enthalpies of the coolant before entering the condenser and at the pinch temperature respectively. The fan or pump isentropic efficiency ($\eta_{p,S}$) is assumed to be 80% and 60% respectively at design point. Finally, the net electrical power output from the WHRS ($\dot{W}_{e,net}$) is as follow:

$$\dot{W}_{e,nett} = \dot{W}_i \cdot \eta_e - \left(\frac{\dot{W}_i + \dot{W}_{i,S}}{\eta_e}\right) \quad (10)$$

3.3. Emission reductions

To quantify the WHRS CO_2 emission reductions (CS_{WHRS}), the operating profile shown in Table 2 will be used for a time span (Δt) of 100 hour:

$$CS_{WHRS}(T_{test}) = \Delta t \cdot CF \cdot (\dot{W}_{AE} \cdot SFOC_{gen,d} - \dot{W}_{e,nett}(T_{test}) \cdot SFOC_{gen}(Load)) \quad (11)$$

Where T_{test} are the 10 different ambient air (seawater) temperatures: -10°C, -5°C, 0°C, 5°C, 10°C, 15˚C, 20°C, 30°C, 40°C, 45°C (1°C, 4°C, 7°C, 11°C, 14°C, 17˚C, 20°C, 27°C, 33°C, 36°C). These are representative of the ambient temperatures encountered around the globe in navigable (i.e. no ice) waters. The auxiliary power demand is represented by $\dot{W}_{AE}$, *CF* stands for carbon factor which it is assumed to be 3.11 g CO_2/g fuel (Smith et al. 2014), $SFOC_{gen,d}$ is the auxiliary engine SFOC at design point while $SFOC_{gen}$ it's the SFOC at off-design operation given in MAN Diesel & Turbo (2013) and referenced to 227 g/kWh at design point. *Load* is used for representing the auxiliary engine loading when the WHRS is installed.

3.4. Optimisation

The models of both the WHRS and condenser unit require up to 14 different variables to be explored with the aim of reducing the ship's CO_2 emissions. The total CO_2 savings will be obtained by using the operating profile shown in Table 2 for a time span of 100 hours for each of the test ambient temperatures. The optimisation approach for this multi-dimensional space is a two-step single objective: Particle Swarm Optimisation (PSWO) followed by Pattern Search Optimisation (PSO). The first optimisation, PSWO (Kennedy & Eberhart 1995), begins with a random distributed data points and looks for the optimum result at each iteration by using gradients or derivatives. In the second step, PSO starts with a reference point in the search space, provided by PSWO, and uses two different search approaches: Exploratory and Pattern. The Exploratory move searches for an improving direction by creating nodes of fixed distance from the reference point and evaluates the function on those new nodes. Pattern improves the search time by increasing the distance to the reference point in the successful direction of the Exploratory move. For more detail please refer to Suárez de la Fuente (2016).

3.5. Model validation

The WHRS thermodynamic model and seawater condenser unit were used in Larsen, Pierobon, et al. (2013), Pierobon et al. (2013) and Pierobon and Haglind (2014) works. There was a 1% difference on the heat exchanger overall heat transfer coefficient when compared to Richardson and Peacock (1994). The air condenser model gave an error of 0.5% and 0.3% for the outlet temperature and the logarithmic temperature difference respectively when compared to Gnielinski (2010).

4. Results

The ORC unit's net electric power production and availability changes depending on the design and operational ambient air temperature, ship speed and coolant. Below 90% the design speed (21.0 kn), none of the designs shown in Fig. 3 operate due to a low enthalpy drop at the expander or temperature cross over at the boiler due to the scavenge air temperature.

Looking at the different design ambient air temperatures, WHRS designed for winter conditions absorb less waste heat than their counterparts, ISO and Tropical, due to a lower temperature at the scavenge air, but thanks to a larger temperature difference between scavenge air and the coolant, the ORC unit becomes more efficient. On the other hand, at higher design ambient air temperatures the WHRS are more inefficient, requiring larger amounts of waste heat to maximise the ship's CO_2 emissions. Contrary to this assertion, the case when air is used as coolant and designed at tropical conditions absorbs less waste heat from the scavenge air. The reason behind this is that the fan power input deducts a considerable part of the WHRS power production – as much as 35% at the higher ambient air temperatures – due to heat rejection to the coolant. The optimisation process, which looks into the highest CO_2 emissions reduction at different ambient air temperatures, prefers an ORC unit which absorbs less waste heat that avoids the fan's power penalty, allowing the air-cooled WHRS to operate in a wider range of operative temperatures. But interestingly, it is seen from Fig. 3E that this WHRS design will not be operating for its design temperature and high ship speed since there is a high fan power requirements and large pressure drops in the condenser unit which fall out the recommended limits (Sinnott 2005).

Regarding operational ambient air temperatures, a similar pattern as with design temperature is seen: as the operational ambient air temperature increases so does the waste heat absorption and hence the coolant's fan/pump power input. For the air-cooled designs the fan power increment due to higher operational temperatures is compensated by a larger amount of waste heat absorbed, having an almost constant power production at a fixed operational speed. In the case of seawater designs, the pump power input has a lesser effect on the net power production; as seen in Fig. 3 B, D and F, in general, these designs have higher net power production as the ambient air temperature increases for the different operational speeds where the WHRS is active.

Comparing both coolants, ORC units cooled by seawater absorb more waste heat from the scavenge air than in the case of air. Interestingly, the air-cooled WHRS produce power in a larger set of ship speeds when the operative ambient air temperature is low. In the particular case of a design ambient air temperature of 10°C (see Fig. 3A and 3B), the air-cooled design produces power for ship speeds between 95% and 105% of the design speed while seawater-cooled operates only at 100% and 105% for operative temperatures below 5°C. For both coolant cases, the low pressure saturation temperature was calculated with the maximum pinch point temperature difference (i.e. 25°C) allowing the designs to operate in a wider range of operative temperatures. Furthermore, seawater temperatures tend to be lower than air temperatures as the ambient air temperature increases which, under this

paper assumption, means that above 20°C seawater will be found colder than air. This temperature behaviour allows marine seawater-cooled WHRS to operate at the highest end of the tested ambient air temperature while air-cooled designs will need to be turn off due to the high power cost.

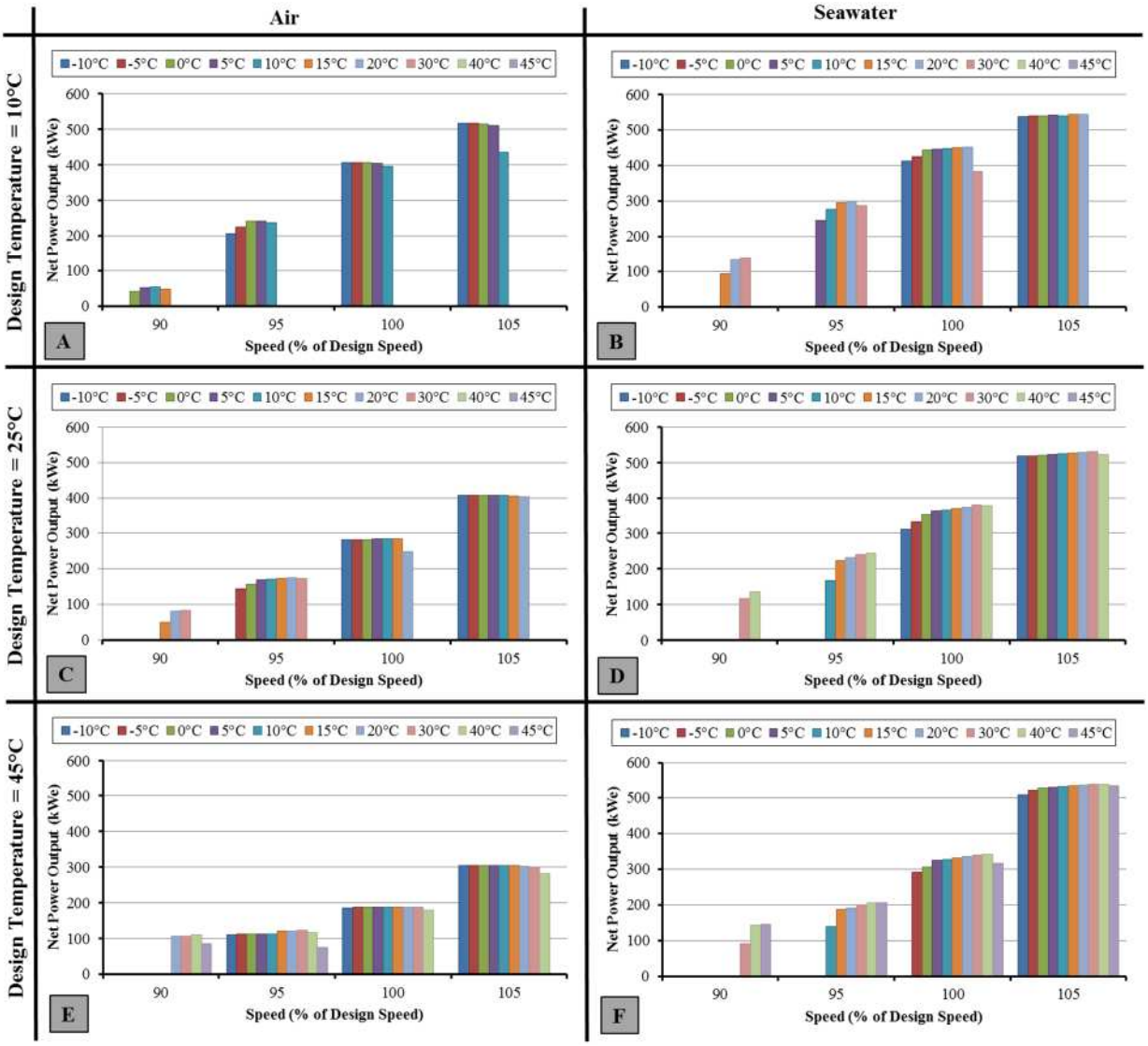

Fig. 3. Net electric power produced by marine WHRS at different operating speeds. A), C) and E) air-cooled at a design ambient air temp of 10°C 25°Cand 45°C; B), D) and F) seawater-cooled at a design ambient air temperature of 10°C, 25°C and 45°C;

Fig. 3 helps to visualise under what operative conditions and coolant the ORC unit returns the highest electric power to the ship. By adding the operating profile from Table 2 to the data shown in Fig. 3 it is possible to calculate the CO_2 emission reductions. The auxiliary engine without the support of the WHRS emits about 98.3 t of CO_2 every 100 hours From Fig. 4 it is possible to see that winter ORC unit designs reduce more the ship's emissions under low and medium ambient air temperatures. In particular winter air-cooled designs outperforms liquid-cooled designs up to an ambient temperature of 5°C and its emission reductions are almost identical to winter seawater designs at 10°C. On the other hand, tropical ambient air temperature designs have the lowest CO_2 emission reductions but, as said before, they can operate over a wider range of ambient air temperatures.

The maximum net CO_2 emission reduction after 100 hours of operation is achieved by seawater-cooled WHRS design for winter conditions at 62.4 t surpassing the 59.6 t of the more flexible tropical condition ORC unit. The larger emission reduction from the winter design is caused by its higher power output and the fact that the WHRS will not be operating just for temperatures above 30°C. For the air, both ISO and tropical designs achieve a similar ship's emission reduction at about 42.1 t of CO_2 while the winter design reaches 40.9 t, being detrimental that it cannot operate at ambient air temperatures above 15°C.

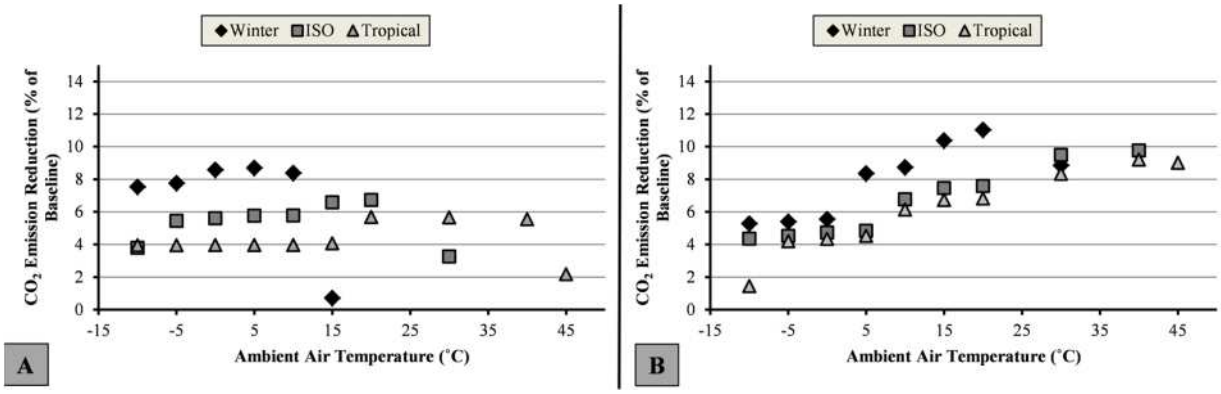

Fig. 4. CO_2 emission reduction as percentage of total auxiliary engine CO_2 emissions and assuming the ship operates 100 hours under each tested ambient air temperature. A) Air; B) Seawater.

Another important difference between air-cooled and seawater-cooled ORC units is the volume of the condenser unit. For the seawater-cooled WHRS the condenser unit volumes are between 6.1 m^3 and 8.0 m^3 while for air-cooled designs the range is between 37.7 m^3 and 38.2 m^3. The larger volumes for air condenser units is due to the lower overall heat transfer coefficient but also to the expensive power cost related to the pressure drop on the air side which goes from 1 Pa to 160 Pa for all air-cooled designs and all ambient air temperatures. For the seawater case the pressure drops are between 103 Pa and 4,220 Pa.

5. Discussion

The maximum power returned to the ship is about 545 kW_e which represents about 33% of the maximum power output of a single auxiliary engine. In regards to CO_2 emissions, the vessel without an ORC installed, under ISO conditions and operative time will be emitting about 955.3 t and 98.3 t for the main and auxiliary engine respectively. The maximum CO_2 emission reductions from any ORC design was 10.8 t which represents about 1.0% of the total vessel's emissions. The proportion of emissions reduced may seem low but it is important to consider that the waste heat source is found at low/medium temperatures which reduce the thermal efficiency of the plant. Rehmatulla (2012) shows that the most common barrier from ship owners for installing any EEED on board is the lack of reliable information on cost and savings. As mentioned before, EEED and ships are normally designed for a particular design point where they offer the highest efficiency. As demonstrated in this work, the performance of a WHRS, depending on the ship speed and ambient air temperature, change. Considering the 10 tested ambient air temperatures, and hence 1,000 hours in operation, the total CO_2 emissions reductions from the winter and seawater-cooled ORC unit reduces to 0.6%. This highlights the importance of considering the operating conditions and profile during the EEED design process. In the particular case of shipping, recognising the impact of weather and off-design operation in the marine WHRS performance could move manufacturers from the most common off-the-shelf to a tailor-made approach, generating more confidence for EEED among ship owners.

6. Conclusions

With the use of a hypothetical 4,130 TEU containership powered by a two-stroke slow speed Diesel engine it was possible to test the performance of different ORC unit designs at off-design conditions with the aim of reducing the ship's CO_2 emissions. It was found that a maximum CO_2 emission reduction representing 1.0% of the total ship's emission is possible using a single ambient air temperature. When having different ambient air temperatures, the vessel's CO_2 emission reduced to 0.6%. If the ship is going to operate under low ambient air temperatures in the majority of its operational life, then a low design temperature and using air as coolant can bring the largest benefit. On the other hand, if the ship will be navigating in long routes throughout the year a seawater-cooled WHRS with high design ambient air temperature can give great operational flexibility. However, it is important to consider that an air condenser unit will occupy up to six times more volume than a seawater condenser.

7. References

Banks C, Turan O, Incecik A, Theotokatos G, Izkan S, Shewell C, Tian X. 2013. Understanding ship operating profiles with an aim to improve energy efficient ship operations. In: Low Carbon Shipp Conf. London; p. 11.

Bustamante JG, Rattner AS, Garimella S. 2016. Achieving near-water-cooled power plant performance with air-cooled condensers. Appl Therm Eng. 105:362–371.

Calleya J, Pawling R, Greig A. 2015. Ship impact model for technical assessment and selection of Carbon dioxide Reducing Technologies (CRTs). Ocean Eng. 97:82–89.

Clarkson Research Services Limited. 2013. Shipping Intelligence Network.

Datla BV, Brasz J. 2014. Comparing R1233zd and R245fa for Low Temperature ORC Applications. In: Int Refrig Air Cond Conf. Purdue: Purdue University; p. 7.

Fakheri A. 2003. A General Expression for the Determination of the Log Mean Temperature Correction Factor for Shell and Tube Heat Exchangers. J Heat Transfer. 125:527.

Gnielinski V. 1976. New Equations for Heat and Mass Transfer in Turbulent Pipe and Channel Flow. Int J Chem Eng. 16:359–368.

Gnielinski V. 2010. G7 Heat Transfer in Cross-flow Around Single Rows of Tubes and Through Tube Bundles. In: VDI-Gesellschaft Verfahrenstechnik und Chemieingenieurwesen, editor. VDI Heat Atlas 2nd ed. Düsseldorf: Springer-Verlag Berlin Heidelberg; p.725–730.

Honeywell. 2014. Solstice ® 1233zd (E) Safety Data Sheet. :1–14.

Hulse RJ, Basu RS, Singh RR, Thomas RHP. 2012. Physical Properties of HCFO-1233zd(E). J Chem Eng Data. 57:3581–3586.

International Maritime Organization. 2009. SOLAS, Consolidated Edition 2009. 5th ed. London: IMO Publishing.

Jones PD, Lister DH, Osborn TJ, Harpham C, Salmon M, Morice CP. 2012. Hemispheric and large-scale land-surface air temperature variations: An extensive revision and an update to 2010. J Geophys Res. 117:D05127.

Jones PD, New M, Parker DE, Martin S, Rigor IG. 1999. Surface air temperature and its changes over the past 150 years. Rev Geophys. 37:173.

Kennedy J, Eberhart R. 1995. Particle swarm optimization. In: Proc ICNN'95 - Int Conf Neural Networks. Vol. 4. Perth: IEEE; p. 1942–1948.

Kontomaris K. 2014. HFO-1336mzz-Z: High Temperature Chemical Stability and Use as A Working Fluid in Organic Rankine Cycles. In: Int Refrig Air Cond Conf. Purdue: Purdue University; p. 10.

Larsen U, Haglind F, Oskar S. 2013. A comparison of advanced heat recovery power cycles in a combined cycle for large ships. In: 26th Int Conf Effic Cost, Optim Simul Environ Impact Energy Syst. Guilin: Chinese Society of Engineering Thermophysics; p. 13.

Larsen U, Pierobon L, Haglind F, Gabrielii C. 2013. Design and optimisation of organic Rankine cycles for waste heat recovery in marine applications using the principles of natural selection. Energy. 55:803–812.

Lemmon EW, Huber ML, McLinden MO. 2010. NIST Reference Fluid Thermodynamic and Transport Properties Database.

Livanos GA, Theotokatos G, Pagonis D-N. 2014. Techno-economic investigation of alternative propulsion plants for Ferries and RoRo ships. Energy Convers Manag. 79:640–651.

MAN Diesel & Turbo. 2005. Thermo Efficiency System for Reduction of Fuel Consumption and CO2 Emission. :16.

MAN Diesel & Turbo. 2012. Waste Heat Recovery System (WHRS) for Reduction of Fuel Consumption, Emission and EEDI. Copenhagen.

MAN Diesel & Turbo. 2013. L32/40 Project Guide - Marine. :278.

MAN Diesel & Turbo. 2014a. Influence of Ambient Temperature Conditions. :17.

MAN Diesel & Turbo. 2014b. MAN B&W G95ME-C9.5-TII Project Guide Electronically Controlled Two-stroke Engines. :329.

MAN Diesel & Turbo. 2015. Engine room and performance data for 8S90ME-C9.5-TII with high load tuning. :10.

Molés F, Navarro-Esbrí J, Peris B, Mota-Babiloni A, Barragán-Cervera Á, Kontomaris K (Kostas). 2014. Low GWP alternatives to HFC-245fa in Organic Rankine Cycles for low temperature heat recovery: HCFO-1233zd-E and HFO-1336mzz-Z. Appl Therm Eng. 71:204–212.

Müller-Steinhagen H, Heck K. 1986. A simple friction pressure drop correlation for two-phase flow in pipes. Chem Eng Process Process Intensif. 20:297–308.

Petukhov BS. 1970. Heat transfer and friction in turbulent pipe flow with variable physical properties. Adv Heat Transf. 6.

Pierobon L, Haglind F. 2014. Design and optimization of air bottoming cycles for waste heat recovery in off-shore platforms. Appl Energy. 118:156–165.

Pierobon L, Larsen U, Haglind F, Elmegaard B, Nguyen T-V. 2013. Multi-objective optimization of organic Rankine cycles for waste heat recovery: Application in an offshore platform. Energy. 58:538–549.

Rayner NA, Brohan P, Parker DE, Folland CK, Kennedy JJ, Vanicek M, Ansell TJ, Tett SFB. 2006. Improved analyses of changes and uncertainties in sea surface temperature measured in situ since the mid-nineteenth century: the HadSST2 data set. J Clim. 19:446–469.

Rehmatulla N. 2012. Barriers to uptake of energy efficient operational measures: Survey Report. London.

Richardson JF, Peacock DG. 1994. Coulson and Richardson's Chemical Engineering Volume 3 - Chemical and Biochemical Reactors and Process Control. 3rd ed. Richardson JF, Peacock DG, editors. Oxford: Elsevier.

Schmidt TE. 1949. Heat transfer calculations for extended surfaces. Refrig Eng. 4:351–357.

Shah MM. 1979. A general correlation for heat transfer during film condensation inside pipes. Int J Heat Mass Transf. 22:547–556.

Shah RK, Sekulic DP. 2003. Fundamentals Of Heat Exchanger Design. 1st ed. New Jersey: John Wiley & Sons, Inc.

Sinnott RK. 2005. Heat-transfer Equipment. In: Coulson Richardson's Chem Eng Vol 6 - Chem Eng Des. 4th ed. Oxford: Elsevier; p.634–793.

Smith TWP, Jalkanen JP, Anderson BA, Corbett JJ, Faber J, Hanayama S., O'Keeffe E., Parker S., Johansson L., Aldous L., et al. 2014. Third IMO GHG Study 2014. London.

Suárez de la Fuente S. 2016. Reducing Shipping Carbon Emissions under Real Operative Conditions: A Study of Alternative Marine Waste Heat Recovery Systems based on the Organic Rankine Cycle. PhD thesis, Dept Mechanical Engineering UCL.

Suárez de la Fuente S, Greig A. 2015. Making shipping greener: comparative study between organic fluids and water for Rankine cycle waste heat recovery. J Mar Eng Technol. 14:70–84.

Suárez de la Fuente S, Roberge D, Greig AR. 2017. Safety and CO2 emissions: Implications of using organic fluids in a ship's waste heat recovery system. Mar Policy. 75:191–203.

Wang C-C, Lee C-J, Chang C-T, Lin S-P. 1999. Heat transfer and friction correlation for compact louvered fin-and-tube heat exchangers. Int J Heat Mass Transf. 42:1945–1956.

Woodyard D. 2009. Pounder's Marine Diesel Engines and Gas Turbines. 9th ed. Oxford: Butterworth-Heinemann.

Yang M-H, Yeh R-H. 2015. Thermo-economic optimization of an organic Rankine cycle system for large marine diesel engine waste heat recovery. Energy. 82:256–268.